Scientific Visualization, 2024, volume 16, number 4, pages 59 - 66, DOI: 10.26583/sv.16.4.06

Adaptation of the Gauss-Newton Optimization Algorithm in Hilbert Diagnostics Using the Bunsen Flame as an Example

E.V. Arbuzov[1,A,C], Yu.N. Dubnishchev[2,B,C], O.S. Zolotukhina[3,B,C]

[A] Sobolev Institute of Mathematics SB RAS
[B] Kutateladze Institute of Thermophysics SB RAS
[C] Novosibirsk State Technical University

[1] ORCID: 0000-0001-9488-8650, arbuzov@math.nsc.ru
[2] ORCID: 0000-0001-7874-039X, dubnistchev@itp.nsc.ru
[3] ORCID: 0000-0003-3486-4459, melexina-olga17@yandex.ru

Abstract

The paper suggests a new form of visualization of the current psycho-emotional and The possibility of using the Gauss-Newton optimization algorithm in Hilbert diagnostics of reacting media (flames) is considered in the paper using the example of data on the temperature and main compounds of a laminar methane-air Bunsen flame. The method of reconstructing phase optical density fields is used to solve the inverse problem of Hilbert optics (it was previously proposed and tested on numerical models): the hilbertogram is calculated in the considered flame axisymmetric section, from which the initial values of the phase function and the medium refractive index are reconstructed. The applications scope expansion of the obtained results in the experimental data processing will be the work development.

Keywords: Hilbert optics, Gauss-Newton algorithm, optimization, Bunsen flame, flame diagnostics.

1. Introduction

Research into combustion processes is relevant in many areas of industry and technology [1, 2]. Optical diagnostics of thermodynamic and structural parameters of flames is the most significant. Non-contact use and the ability to take measurements in high-temperature zones are its main advantages. Optical diagnostic methods can be conditionally divided into two groups: approaches based on the scattering phenomena, absorption and fluorescence during the light radiation passage through the medium under study constitute the first [3–5]; methods that consist of recording changes in the refractive index (phase density) of a gas mixture belong to the second [6, 7].

Optical Hilbert diagnostics allows for highly sensitive visualization of phase structures of the media being studied in a space limited by a probing light field [8]. The results of polychromatic Hilbert diagnostics of hydrogen-air diffusion flame with reconstruction from the obtained phase function of the temperature field and determination of the combustion products concentrations were presented earlier in [9]. However, the issue of phase fields automatic calculation based on Hilbert measurement data remains unresolved.

The use of the iterative Gauss-Newton algorithm, which is applied to find the minimum of the objective function [11, 12], was proposed in [10] using the example of numerical models for optimizing the phase function reconstruction in Hilbert diagnostics. The adaptation of Gauss-Newton optimization to the solution of the inverse Hilbert-optics problem using experimental data on the temperature and main compounds of the laminar methane-air Bunsen flame described in [13] is performed in the present work.

2. Optimization problem

A mathematical model of Hilbert visualization of phase disturbances in a certain section y of the diagnosed object (the z axis coincides with the light beam direction) can be given by the relation [10]:

$$H[\psi](x^*, y) = \left\{\int_{-\infty}^{+\infty} \frac{\cos[\psi(x,y)]}{x^* - x} dx\right\}^2 + \left\{\int_{-\infty}^{+\infty} \frac{\sin[\psi(x,y)]}{x^* - x} dx\right\}^2. \quad (1)$$

The function $\psi(x, y)$ in turn depends on the geometric path length and the refractive index $n(x, y, z)$:

$$\psi(x,y) = \frac{2\pi}{\lambda} \int_{z_1}^{z_2} [n(x,y,z) - n_\infty] dz, \quad (2)$$

where λ is the wavelength, n_∞ is the refractive index of the medium surrounding the flame, z_1 and z_2 are the initial and final points of light beam propagation in the object. Expression (2) can be represented through the Abel integral [9] in the case of axial symmetry:

$$\psi(x,y) = \frac{4\pi}{\lambda} \int_x^R [n(r,y) - n_\infty] \frac{r}{\sqrt{r^2 - x^2}} dr\,;\; r^2 = x^2 + z^2; \quad (3)$$

R is the radius of the flame axisymmetric cross-section; $n(r, y)$ is the dependence of the refractive index on the radius within the cross-section.

The relationship between the refractive index and the burning mixture parameters is determined by the ratio:

$$n - 1 = \frac{p}{p_{n.c.}} \frac{T_{n.c.}}{T} \sum_k A_k \left(1 + \frac{B_k}{\lambda^2}\right) C_k, \quad (4)$$

where p is the pressure in the flame spatial structure; $p_{n.c.}$ is the pressure under normal conditions; T is the flame temperature; $T_{n.c.}$ is the temperature under normal conditions; C_k is the mole fraction of the k-th component of the burning mixture; A_k and B_k are the dispersion coefficients of the k-th component of the burning mixture (reference data). The phase function $\psi(x, y)$ from the hilbertogram $H[\psi]$ must be reconstructed to find the flame parameters under study T and C_k.

Using numerical models as an example, the authors proposed in [10] a method based on the iterative Gauss-Newton algorithm for automatically performing this operation. The method consists of selecting a phase profile specified by the sum of third-degree Bezier curves [14], then calculating the hilbertogram and comparing it with experimental data. The structures coincidence of the experimental and model hilbertograms serves as a criterion for the reconstruction reliability of $\psi(x, y)$.

If we set some phase function initial approximation through a sections set, each of which is modeled by a Bezier curve:

$$\psi_q^{mod}(x,y): \begin{cases} x\left(t, V_x^q\right) = (1-t)^3 V_{x,o}^q + 3(1-t)^2 t V_{x,1}^q + 3(1-t) t^2 V_{x,2}^q + t^3 V_{x,3}^q \\ y\left(t, V_y^q\right) = (1-t)^3 V_{y,o}^q + 3(1-t)^2 t V_{y,1}^q + 3(1-t) t^2 V_{y,2}^q + t^3 V_{y,3}^q \end{cases};$$
$$t \in [0,1];$$

where V_x^q and V_y^q are the vectors components of the Bezier curve support vertices with the number $(q = 1, \dots, Q)$, and calculate $H^{mod}[\psi^{mod}]$ from it, then the optimization problem is reduced to determining V_x^q and V_y^q, at which the objective function minimum is achieved:

$$f(\vec{V}) = \left\|F(\vec{V})\right\|^2 = \sum_{m=0}^{M} [H(x_m) - H^{mod}(x_m)]^2.$$

Iterative approximations are performed to find $\vec{V}$:

$$\overrightarrow{V_{d+1}} = \overrightarrow{V_d} - \alpha\left[J^T\left(\overrightarrow{V_d}\right) J\left(\overrightarrow{V_d}\right)\right]^{-1} J^T\left(\overrightarrow{V_d}\right) F\left(\overrightarrow{V_d}\right), \quad (5)$$

where α is the iteration step adjustment coefficient, J is the Jacobian matrix of first-order derivatives of the function $F(\vec{V})$. As a result, optimization consists of specifying a vector $\overrightarrow{V_0}$ that

determines the initial distribution $\psi(x, y)$, and then applying the Gauss-Newton algorithm (5) until the distances squares sum between the coordinates of the experimental and optimized hilbertograms becomes less than the specified value.

3. Experimental data processing

Let us turn to Fig. 1.*a* and 1.*b*, which show the radial distribution of temperature T and molar concentrations of fuel combustion products C_{N_2}, C_{O_2}, C_{H_2}, C_{H_2O}, C_{CO_2}, C_{CO} and C_{CH_4} in some sections y_1 and y_2 of a laminar methane-air Bunsen flame. The data are taken from the work [13], in which they were obtained using Raman-Rayleigh scattering and laser-induced fluorescence methods.

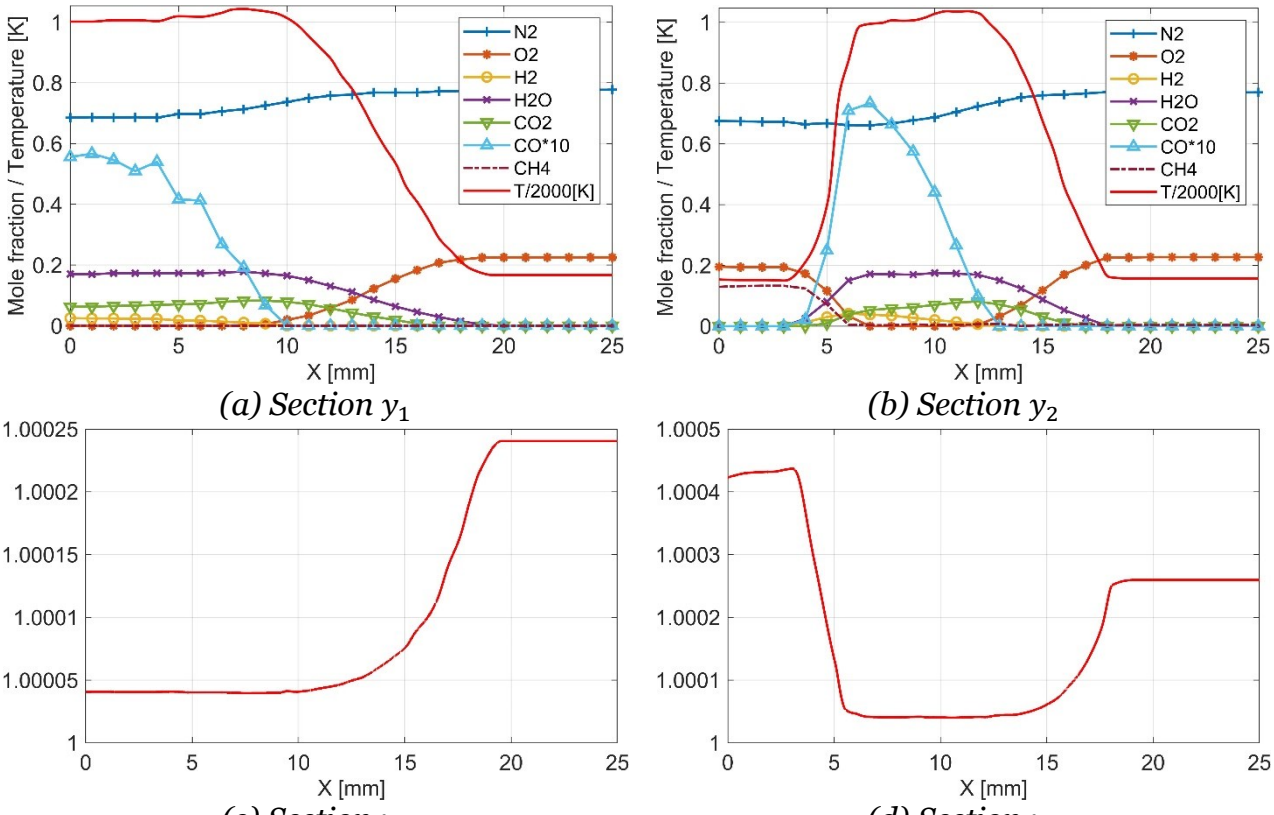

(a) Section y_1 *(b) Section y_2*

(c) Section y_1 *(d) Section y_2*

Fig. 1. (*a, b*) Radial distribution of temperature and molar concentrations of fuel combustion products; (*c, d*) radial distribution of refractive index.

The value of C_{CH_4} is defined as follows:

$$C_{CH_4} = 1 - C_{N_2} - C_{O_2} - C_{H_2} - C_{H_2O} - C_{CO_2} - C_{CO}.$$

Using the obtained data, we calculate the refractive index in the flame sections under consideration according to (4) at λ = 532 nm and $p = p_{n.c.}$ (Fig. 1.*c* and 1.*d*). Then, applying formulas (3) and (1), we find the phase function ψ and the corresponding hilbertogram $H[\psi]$ (Fig. 2).

The inverse problem of Hilbert diagnostics is to reconstruct ψ from the recorded hilbertogram $H[\psi]$ in experimental measurements. The Hilbert transform allows visualization of the extremes and gradients of the phase optical density of the studied medium, which are transformed into Hilbert band structures, with "wide" bands being formed in the region of extremes [8]. We use this information to specify some initial approximation ψ^{mod} and $H^{mod}[\psi^{mod}]$, which must be optimized to the "reference" values (Fig. 3). Since the flame is axisymmetric, for the first section y_1 it was necessary to use three Bezier curves and display their copies relative to the central axis, for the second section y_2 – 5 curves.

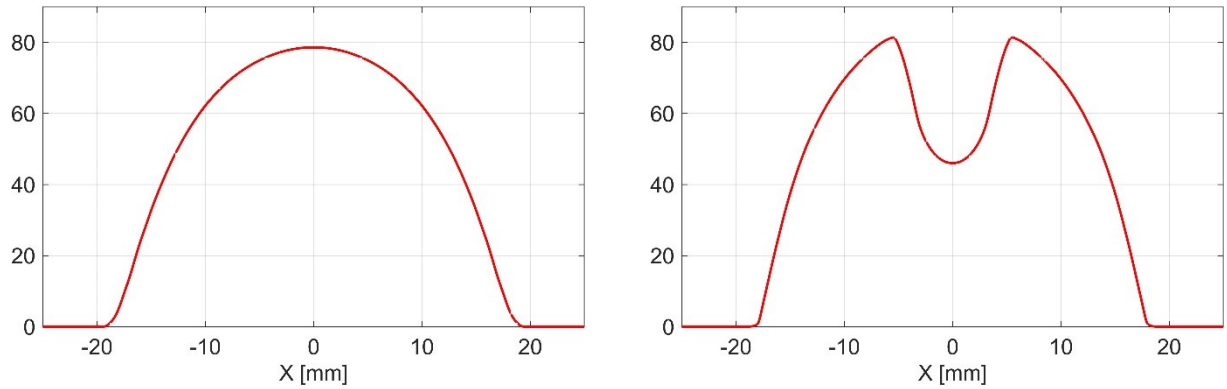

(a) Section y_1 *(b) Section y_2*

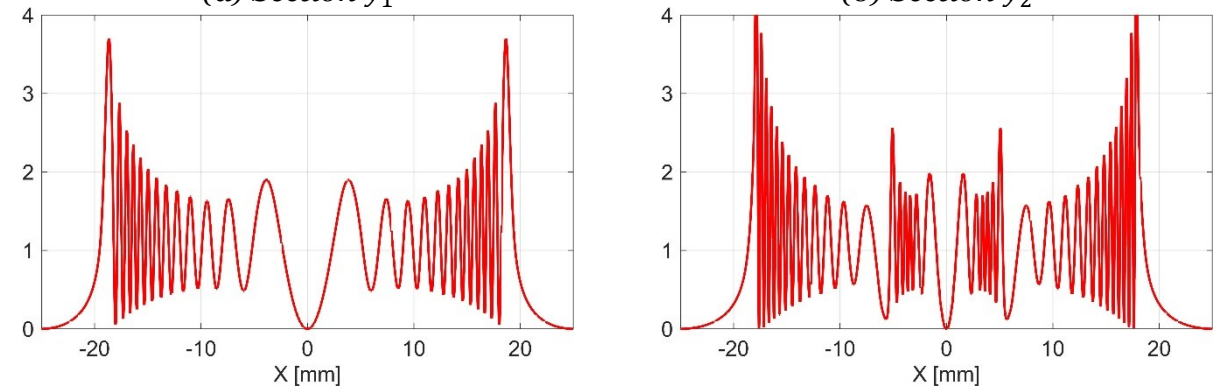

(c) Section y_1 *(d) Section y_2*

Fig. 2. Reference data: (*a, b*) phase function; (*c, d*) hilbertogram.

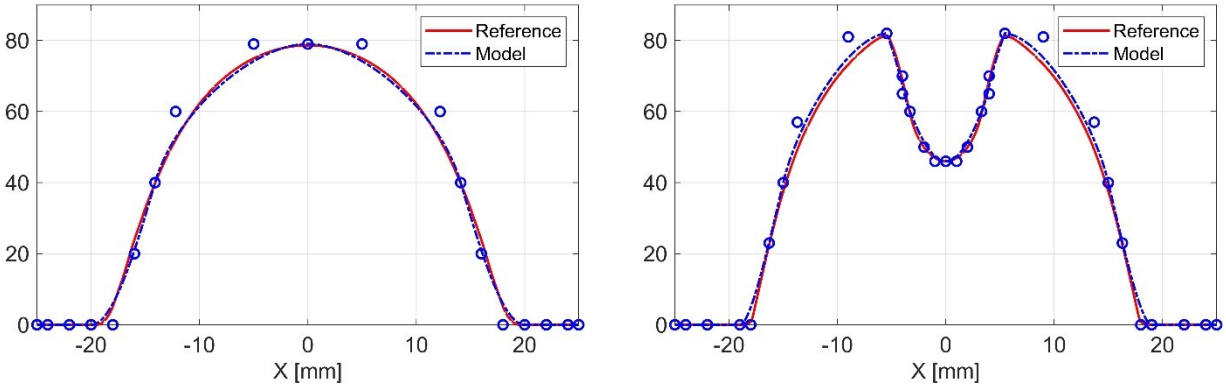

(a) Section y_1 *(b) Section y_2*

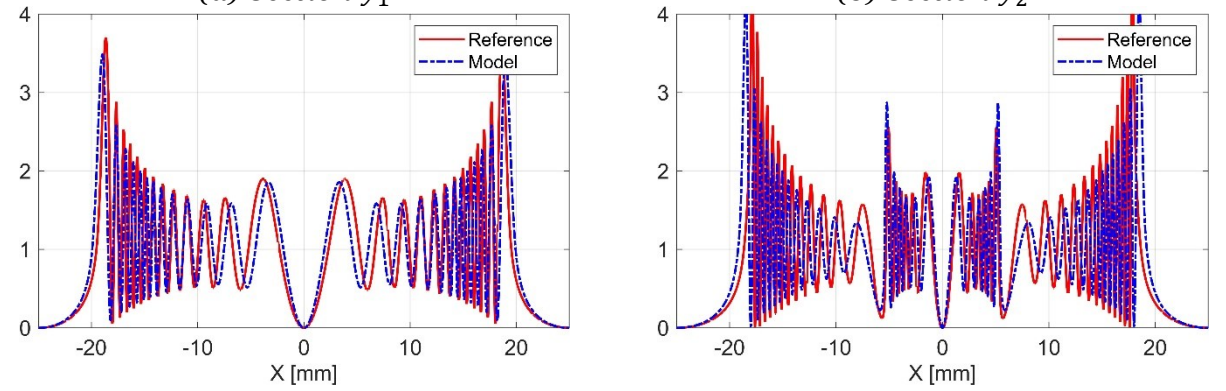

(c) Section y_1 *(d) Section y_2*

Fig. 3. Initial approximation: (*a, b*) phase function represented by the Bezier curves sum (with specified reference vertices); (*c, d*) hilbertogram.

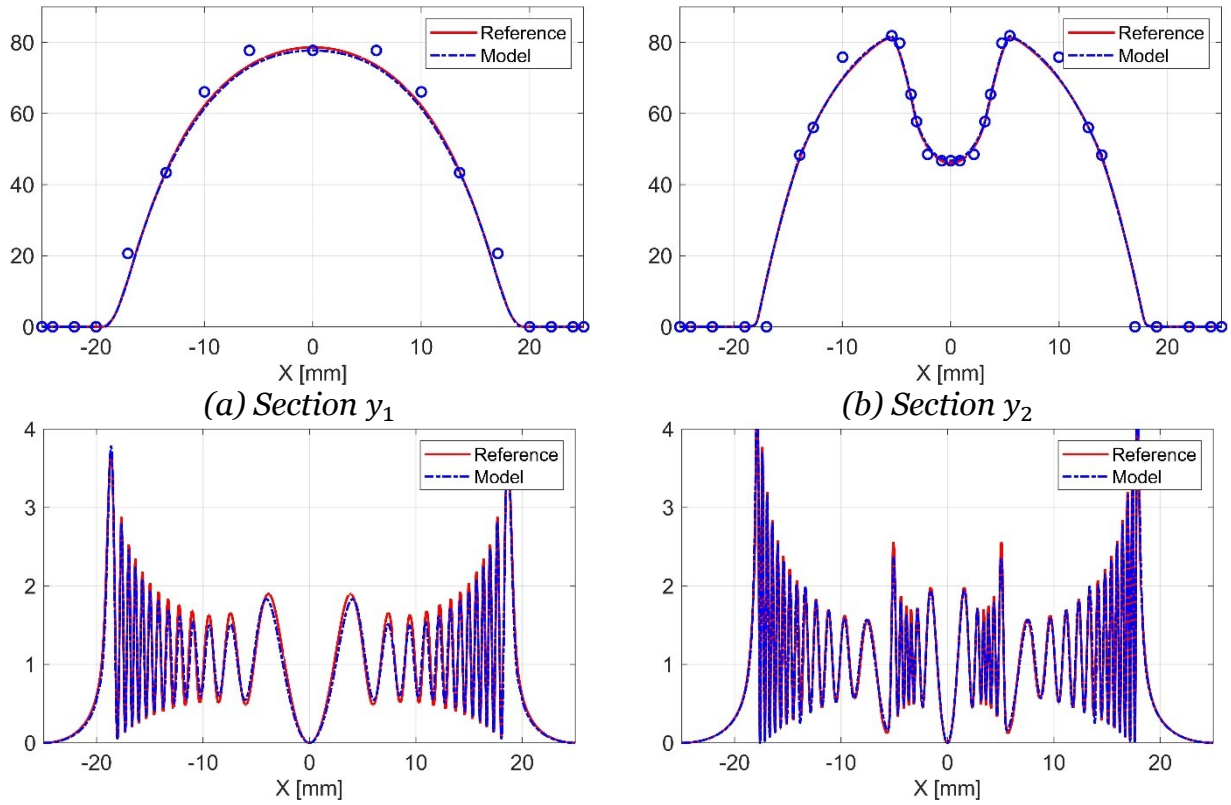

(a) Section y_1 *(b) Section y_2*

(c) Section y_1 *(d) Section y_2*

Fig. 4. Optimization result: (*a, b*) phase function; (*c, d*) hilbertogram.

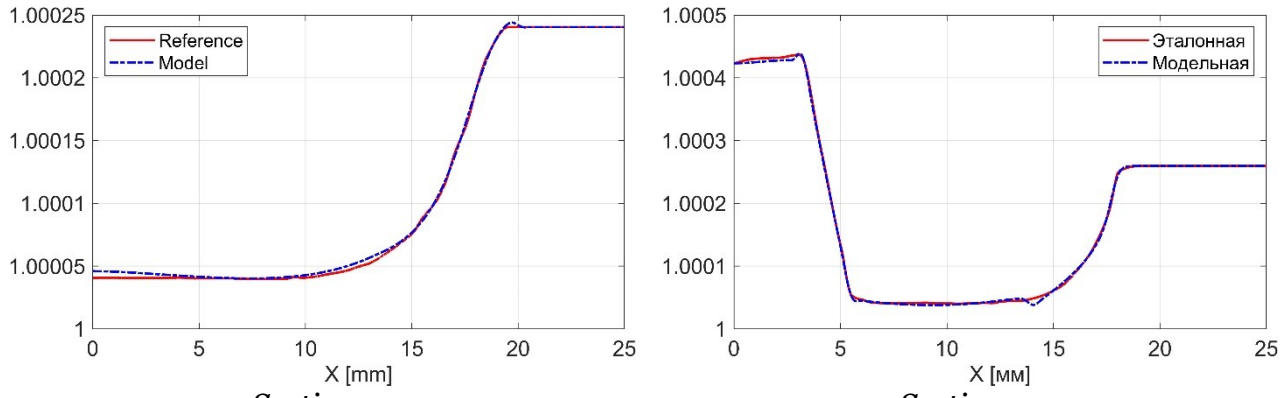

Section y_1 *Section y_2*

Fig. 5. Comparison of the refractive index initial distribution (Fig. 1.*c* and 1.*d*) in the flame sections y_1 and y_2 with that reconstructed as a result of solving the inverse Hilbert optics problem.

Let us fix the known coordinates of the polynomials reference vertices: the phase value at the studied region edges and the function extrema location. The result of applying the Gauss-Newton optimization algorithm (5) is shown in Fig. 4. From the phase function reconstructed profile, we calculate the refractive index (Fig. 5) and compare the result with the initial data shown in Fig. 1.*c* and 1.*d*.

4. Discussion of results

The Gauss-Newton optimization algorithm through 52 iterations in the y_1 section and 31 iterations in the y_2 section made it possible to bring the optimized data H^{mod} closer to the reference values H with a root-mean-square error

$$\sigma_{y_1} = \sqrt{\frac{\sum_{m=0}^{M}\left(H_{m,y_1} - H_{m,y_1}^{mod}\right)^2}{M}} = 0{,}12;\ \sigma_{y_2} = \sqrt{\frac{\sum_{m=0}^{M}\left(H_{m,y_2} - H_{m,y_2}^{mod}\right)^2}{M}} = 0{,}11;$$

while the maximum deviation of the reconstructed phase function from the reference one turned out to be localized in the sections central part and amounted to

$$\delta_{\psi,y_1} = \max_{m=0,\dots,M}\left|\psi_{m,y_1} - \psi_{m,y_1}^{mod}\right| = 0{,}88;\ \delta_{\psi,y_2} = \max_{m=0,\dots,M}\left|\psi_{m,y_2} - \psi_{m,y_2}^{mod}\right| = 0{,}37;$$

which is also observed in the refractive index resulting distribution:

$$\delta_{n,y_1} = \max_{m=0,\dots,M}\left|n_{m,y_1} - n_{m,y_1}^{mod}\right| \approx 2{,}5 \cdot 10^{-6};$$

$$\delta_{n,y_2} = \max_{m=0,\dots,M}\left|n_{m,y_2} - n_{m,y_2}^{mod}\right| \approx 1{,}1 \cdot 10^{-5}.$$

As can be seen in Fig. 5, small "spikes" that reflect insufficiently smooth connections between the regions modeled by the Bezier curves are present in the reconstructed data. Therefore, the issue of a more accurate and smooth connection of polynomials when setting the initial approximation and the optimization algorithm operation will be resolved in the future. In addition, an increasing possibility analysis of the reconstruction accuracy in the studied sections central part is necessary, which is associated with the Hilbert transform property. The introduction of additional a priori information, which allows the Gauss-Newton algorithm to more accurately find the objective function minimum, may be required for this.

Conclusion

Using the data example on the temperature and main molar concentrations of combustion products of a methane-air Bunsen flame, the automatic reconstruction method of phase structures based on Hilbert diagnostics data using the Gauss-Newton optimization algorithm was tested in the work. An iterative selection of the phase function profile, adapted through the third-degree Bezier curves sum, was performed in axisymmetric sections of the flame under study, followed by calculation of the refractive index spatial structure. It has been established that the criterion for the phase reconstruction reliability is the structures coincidence of the reference and model hilbertograms. The optimization accuracy increasing problem, as well as expanding the scope of obtained results applications to the experimental data processing, will be the further research subject.

Acknowledgments

The work was carried out within the framework of the state assignment of IM SB RAS (No. FWNF-2022-0009) and state assignment of IT SB RAS (No. 121031800217-8).

References

1. Li J., Huang H., Bai Y., and etc. Combustion and heat release characteristics of hydrogen/air diffusion flame on a micro-jet array burner // Int. J. Hydrog. Energy., Vol. 43 (29), 2018, pp. 13563–13574 (doi: 10.1016/j.ijhydene.2018.04.195).

2. Masri A. R. Challenges for turbulent combustion // Proc. Combust. Inst., Vol. 38 (1), 2021, pp. 121–155 (doi: 10.1016/j.proci.2020.07.144).

3. Jiang N., Roy S., Hsu P. S., and etc. High-speed, two-dimensional, multi-species Raman imaging for combustion and flow diagnostics // AIAA 2018-2040, 2018. (doi: 10.2514/6.2018-2040).

4. Yang H. N., Yang B., Cai X. S., and etc. Three-dimensional (3-D) temperature measurement in a low pressure flame reactor using multiplexed tunable diode laser absorption spectroscopy (TDLAS) // Laser. Eng., Vol. 31, 2015, pp. 285–297.

5. Gazeli K., Lombardi G., Aubert X., and etc. Progresses on the use of two-photon absorption laser induced fluorescence (TALIF) diagnostics for measuring absolute atomic densities in plasmas and flames // Plasma, Vol. 4 (1), 2021, pp. 145–171 (doi: 10.3390/plasma4010009).

6. Ostrovsky Yu. I., Butusov M. M., Ostrovskaya G. V. Golograficheskaya interferometriya [Holographic interferometry], Nauka Publ., Moscow, 1977, 336 p. (in Russian)
7. Karaminejad S., Askari M. H., Ashjaee M. Temperature field investigation of hydrogen/air and syngas/air axisymmetric laminar flames using Mach-Zehnder interferometry // Appl. Opt., Vol. 57 (18), 2018, pp. 5057–5067 (doi: 10.1364/AO.57.005057).
8. Arbuzov V. A., Dubnishchev Yu. N. Metody gil'bert-optiki v izmeritel'nykh tekhnologiyakh [Hilbert-optics methods in measurement technologies], NSTU University Publ., Novosibirsk, 2007, 316 p. (in Russian)
9. Dubnishchev Yu. N., Arbuzov V. A., Arbuzov E. V., and etc. Optical diagnostics of hydrogen-air diffusion jet flame // J. Eng. Thermophys., Vol. 31 (3), 2022, pp. 402–413 (doi: 10.1134/S1810232822030031).
10. Arbuzov E. V., Arbuzov V. A., and etc. Gauss-Newton method in the problem of optimizing the axisymmetric phase function calculation based on the Hilbert diagnostic data // Scientific Visualization, Vol. 15 (4), 2023, pp. 56–67 (doi: 10.26583/sv.15.4.05).
11. Dennis J. E., Schnabel R. B. Numerical methods for unconstrained optimization and nonlinear equations. Prentice-Hall, Inc., Englewood Cliffs, NJ, 1983, 395 p.
12. Lai W. H., Kek S. L., Tay K. G. Solving nonlinear least squares problem using Gauss-Newton method // Int. J. Innov. Sci., Vol. 4 (1), 2017, pp. 258–262.
13. Nguyen Q. V., Dibble R. W., Carter C. D. Raman-LIF measurements of temperature, major species, OH, and NO in a methane-air Bunsen flame // Combust. Flame., Vol. 105 (4), 1996, pp. 499–510.
14. Bezier curves, 2022. URL: https://learn.javascript.ru/bezier.